Statistical study of effective anisotropy field in ordered ferromagnetic nanowire arrays

Zhao, S.; Clime, L.; Chan, K.; Normandin, F.; Roberge, H.; Yelon, A.; Cochrane, R. W.; Veres, T.

Publisher's version / Version de l'éditeur:
https://doi.org/10.1166/jnn.2007.024
Journal of Nanoscience and Nanotechnology, 7, 1, pp. 1-6, 2007-01-01

Journal of
Nanoscience and Nanotechnology
Vol. 7, 1–6, 2007

Statistical Study of Effective Anisotropy Field in Ordered Ferromagnetic Nanowire Arrays

S. Zhao[1,2], L. Clime[1,2], K. Chan[1,3], F. Normandin[1], H. Roberge[1], A. Yelon[2], R. W. Cochrane[4], and T. Veres[1,*]

[1]*NRC, Industrial Material Institute, 75 Boul. de Mortagne, Boucherville, Canada J4B 6Y4*
[2]*École Polytechnique de Montréal, Département de génie physique and Regroupement québécois sur les matériaux de pointe (RQMP), CP 6079, succursale Centre-ville, Montréal, Québec, H3C 3A7, Canada*
[3]*Simon Fraser University, 8888 University Drive, Burnaby, B.C. Canada. V5A 1S6*
[4]*Département de physique, Université de Montréal, and Regroupement québécois sur les matériaux de pointe (RQMP), CP 6128, succ. Centre-ville, Montréal, Québec, H3C 3J7, Canada*

Soft ferromagnetic nanowire arrays were obtained by electrodeposition of Co–Fe–P alloy into the pores of high quality home-made anodized aluminum oxide (AAO) templates. Bath acidity and current density were the two parameters used in order to tailor the orientation of local anisotropy axes in individual nanowires. In order to quantify the influence of the induced anisotropies on the magnetization processes in individual nanowires, the in-plane magnetization loops of the arrays are modeled as log-normal distributions of Stoner-Wohlfarth transverse magnetization processes. Using the lognormal mean parameter as an approximation for the saturation applied field of the array, we compute the effective anisotropy of the nanowires, which is found to decrease with the pH of the electrodeposition bath.

Keywords: Magnetic Nanostructures, Ferromagnetic Nanowires, Nanowire Arrays, Lognormal Distribution, Anisotropy Field, Electrodeposition

RESEARCH ARTICLE

1. INTRODUCTION

Arrays of ferromagnetic nanowires are of great technological interest and have become very promising systems for the design of high-density perpendicular recording media, logic gates, and magnetic sensors. These arrays may be readily fabricated by electrodeposition of Co, Ni, Fe or their alloys into the pores of various types of templates.[1–7] Zero magnetostrictive compositions and high saturation magnetic inductions of Co–Fe–P alloys[8] open significant opportunities for these materials in ultra-high-density magnetic recording media and various nanotechnological applications such as high frequency metamaterials or sensors. Among the various methods used in preparing of these nanowire arrays, the electrodeposition of magnetic materials in nanoporous host templates is a very convenient approach for producing large arrays of parallel and almost identical nanowires.[7] Along with the geometry of the arrays, the magnetocrystalline anisotropy of the ferromagnetic materials may play a very important role in the magnetization reversal of individual nanowires. Accurate micromagnetic simulations[9–11] have demonstrated that the crystalline structure of Ni and Fe is not important in the static magnetization processes of nanowire arrays, whereas various experimental studies[5, 12, 13] demonstrated the strong influence of the magnetocrystalline axes (MCA) orientation on the magnetization processes in Co-based nanostructures. Moreover, experimental evaluations of MCA distributions by ferromagnetic resonance experiments with electrodeposited Co nanowires[14] have revealed a strong dependence of the magneto-crystalline anisotropy on the bath acidity (pH), this last parameter being widely used for tailoring the *c*-axis orientation in these systems.[14]

We present below a method for obtaining large scale, high quality, CoFeP amorphous nanowire arrays. We use this system to develop and test a statistical approach to the identification of local anisotropy distributions in nanowires using the in-plane magnetization loops of theirs arrays. With the assumption of a log-normal distribution of anisotropy, we estimate the average saturation field of individual nanowires and consequently the average anisotropy field, h_k, using a model for the interaction field at saturation.[15] The main feature of this model is that it does not require accurate information about the inter-wire spacings and it does not need the saturation magnetization or moment at all.[15] However, in order to distinguish between geometrical

*Author to whom correspondence should be addressed.

 1533-4880/2007/7/001/006 doi:10.1166/jnn.2007.024

demagnetizing anisotropy fields of individual nanowires, $M_s/2$, and local intrinsic anisotropy of the ferromagnetic material such as magneto-crystalline or magnetostrictive, accurate values for the saturation magnetization are needed. We apply this approach to CoFeP nanowire arrays with different P content, prepared by electrodeposition into the pores of anodized aluminum oxide (AAO) membranes made in our laboratory. We present the dependence of the P content of the ferromagnetic alloy and the average anisotropy field of individual nanowires on the bath acidity.

2. EXPERIMENTAL SETUP

AAO films were synthesized using the two-step anodization method (0.3 M oxalic acid, 40 V) developed by Masuda and Fukuda.[16] Al 99.999% 0.50 mm foils (Goodfellow Cambridge Ltd.) were first degreased with acetone, etched in 1.0 M NaOH(aq) for about 1 min until bubbles over the surface were observed, and then electropolished in a mixture of C_2H_5OH and $HClO_4$ (3 : 1 v/v). All AAO films were subjected to a first anodization for 4 hours, followed by the dissolution of the oxide layer in a phosphocromic acid solution ($6\%H_3PO_4 + 1.8\%H_2CrO_4$ aqueous solution), and finally by a second anodization for 1 day. The anodization was carried out at 1 °C, with temperature controlled by a cool plate (Stir-Kool SK-12D). A pure Pt foil was used as a cathode. The AAO film was then detached from the Al substrate, by applying a brief voltage pulse in a bath of a 1 : 1 (v/v) mixture of 2,3-butanedione $(CH_3CO)_2$ (98%) and $HClO_4$(aq.) (70%).[17] In this way, an open-through AAO film was obtained with the initial morphology. It is very important to rinse the sample thoroughly with acetone immediately after this step, because the residue from the detachment step, if left on the template for a period of time, seems to affect the adhesion of the electrode layer that needs to be sputtered or evaporated.

Nanowires were grown in the AAO templates using DC electrodeposition.[18] A 450 nm Ag film was sputtered onto the back of the open-through template as the working electrode. Where low pH plating baths were used, a 10 nm Ti adhesion layer was first evaporated onto the membrane, followed by an additional 450 nm layer of Ag, both at a 30° angle of incidence. To assure that plating occurred only within the pores of the AAO membrane, at least 2 layers of photoresist (S-1805) were painted on the back and edges of the sample and its solvent evaporated at 200 °C. All plating took place at room temperature in a two-electrode plating cell, with Pt foil as a counterelectrode. After plating, the photoresist layer was rinsed away with acetone. The CoFeP nanowires were electrochemically deposited at a voltage of 2.6 V for various times, from an electrolyte consisting of $CoSO_4 \cdot 7H_2O$ (112g/l), $FeSO_4 \cdot 7H_2O$(28g/l), $NaH_2PO_2 \cdot H_2O$(22g/l), $H_3BO_3 \cdot 2H_2O$(47g/l), $Na_3C_6H_5O_7$ (Sodium Citrate)21g/l). For Scanning Electron Microscopy (SEM) characterization (Hitachi S-4700) the templates were partially dissolved in 1.0 M NaOH(aq) for ~10 min. Energy Dispersive X-Ray (EDX, Bruker AXS) and X-ray Diffraction (XRD, D8-Discover) measurements were employed in order to study the morphology and the composition of the electrodeposited alloy. A Quantum Design Physical Property Measurement System (PPMS) was used to determine hysteresis loops of the arrays for fields up to 2 Tesla with a resolution of 2×10^{-5} emu.

In what follows, we shall present the relationship between the effective anisotropy of individual nanowires and the IP saturation field of the array. The effective anisotropy is the resultant of the intrinsic anisotropy and the geometric, demagnetizing anisotropy.

3. THEORETICAL MODEL

In earlier work[15, 19] we have shown that the effective anisotropy of the nanowires in an array can be determined from knowledge of the applied field at saturation, H_s. One method[15] determines the effective anisotropy from H_s of IP loops, which as we may observe from Figure 4 resemble transverse (hard direction) Stoner-Wohlfarth loops.[20, 21] This method requires only accurate knowledge of wire length, l, and approximate knowledge of wire spacing, d. That is, no knowledge of saturation magnetization, M_s, nor of wire radius, r, is required. Here, we extend this method, by the introduction of an *ad-hoc* assumption, which we show works remarkably well. This assumption will permit us to make a precise choice of the value of the saturation applied field, H_s, and thus, to improve the precision of our calculation.

The assumption proceeds in several steps. First we assume that the nanowire array may be considered as consisting of elementary, independent objects or particles. We may think of these particles as being the individual wires, or as portions of wires. The global equilibrium magnetization state can be obtained by minimization of the torque exerted on the magnetization of each particle by the local effective field. This field consists of three components, the applied field, H, the interaction field, which is on average parallel to the applied field, and the effective anisotropy field, which itself consists of two parts, intrinsic and demagnetizing, as discussed above.

Now, we define the particle anisotropy field as the resultant of the local effective anisotropy field and the local interaction field. In all realistic cases of transition metals and their alloys in nanowire arrays, the membrane plane will be hard for individual wires. Even in the case of mono-crystalline Co with c-axis in the plane, the magnetocrystalline anisotropy field is only half of the demagnetizing field,[10, 11] and the interaction field at saturation will be a fraction of $M_s/2$. We note, however, that for the array it is possible for saturation IP to occur at lower field than for OOP, since the OOP interaction field opposes the applied field. Thus, in-plane magnetization processes can still be considered as a superposition of elementary

RESEARCH ARTICLE

transverse Stoner-Wohlfarth magnetization loops:[20, 21]

$$m(H_{kp}; H) = \begin{cases} +1, & H \geq H_{kp} \\ \dfrac{H}{H_{kp}}, & -H_{kp} < H < +H_{kp} \\ -1, & H \leq -H_{kp} \end{cases} \quad (1)$$

In Eq. (1) m represents the normalized magnetic moment of the particle and H the external (applied plus interaction) field. H_{kp} is the total anisotropy field as given by the competition between the global demagnetizing field of the ferromagnetic cylinder and the local magneto-crystalline anisotropy field. Now, we assume the distribution of H_{kp} well described by the log-normal probability distribution function (PDF):[22]

$$\mathrm{PDF}(H_{k0}, \sigma; H_{kp}) = \frac{1}{H_{kp}\sigma\sqrt{2\pi}} \exp\left\{-\frac{\ln^2(H_{kp}/H_{k0})}{2\sigma^2}\right\} \quad (2)$$

We denoted above the *standard deviation* and the *distribution median* as σ and H_{k0} respectively. Transverse magnetization loops for individual nanowires are then obtained as a superposition of elementary magnetization loops:

$$M(H) = M_0 \int_0^\infty m(H_{kp}; H) \cdot \mathrm{PDF}(H_{k0}, \sigma; H_{kp}) dH_{kp} \quad (3)$$

We must point out that neither H_{k0}, nor any other PDF parameter (the mode or the mean) obtained by fitting of the magnetization loops of the arrays can be directly related to physical properties of individual nanowires because of the interaction field between nanowires. In order to extract the effect of these interactions on the parameter H_{kp}, we use a model for the anisotropy field in individual nanowires.[15] Assuming that the effective anisotropy is independent of l, we have shown that above a small length called dipolar length, typically less than 1 μm, H_s varies linearly with l. IP experimental values of the saturation applied field H_s^{IP} can be well fitted then with linear functions

$$H_s^{\mathrm{IP}}(l) = Al + B \quad (4)$$

where A and B are two fit parameters. From the model, the average effective anisotropy field in individual nanowire is given by

$$\bar{h}_k = B + A\gamma(d) \quad (5)$$

$\gamma(d)$ is a universal function of all extended nanowire arrays[15] and depends only on d. Since γ varies slowly with d over the range of values of d of AAO membranes, the value of γ for a given interwire spacing can easily be determined to better than 3%. We take as the saturation field H_s^{IP} of the array the PDF *mean* parameter:

$$H_s^{\mathrm{IP}} \cong H_{km} = H_{k0} \exp\left\{\frac{\sigma^2}{2}\right\} \quad (6)$$

with H_{k0} and σ as obtained from numerical fit of the experimental in-plane magnetization loops. Using H_s^{IP} values in Eq. (4) we obtain $\bar{h}_k$ from Eq. (5). The use of this procedure permits the elimination of the effect of the interaction field and to extract $\bar{h}_k$, which is independent of l.

4. RESULTS AND DISCUSSION

Using the two-step anodization method as described in Section 2, we obtained large, uniform AAO templates characterized by narrow distributions both of hole diameters and inter-hole spacings (Fig. 1a) and a very good parallelism of the holes' symmetry axes (Fig. 1b). As may be seen from the SEM images of Figure 2, the growth of nanowires was uniform. Arrays containing nanowires with lengths from 1 μm up to 45 μm were obtained by varying the electrodeposition time from tens of minutes to several hours.

EDX measurements (Fig. 2) show that the P content of the nanowires decreases from 21% at pH = 1.5 to 8% at pH = 4.0 (Fig. 3). XRD measurements with Copper K_α radiation, indicate that the electrodeposited alloy is amorphous, although a small nanocrystalline component can not be excluded. Magnetic measurements of the nanowire arrays show low coercivities and high saturation fields in the plane of the array (in-plane, or IP) and higher coercivities and lower saturation fields parallels to the wire axis (out-of-plane, or OOP), as shown in Figure 4.

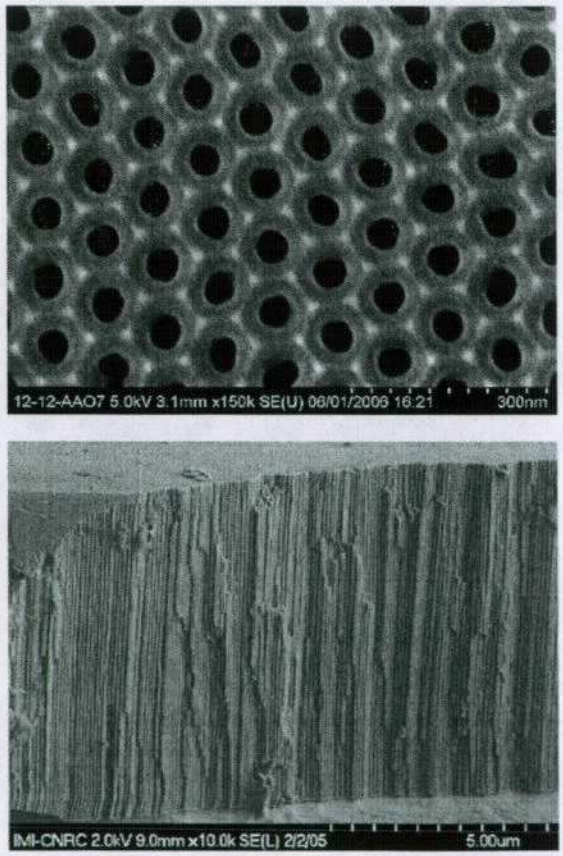

Fig. 1. SEM images of obtained AAO templates: (a) top view; (b) side view of a broken template. The anodization was performed in 0.3 M oxalic acid at 40 V and 1 °C.

RESEARCH ARTICLE

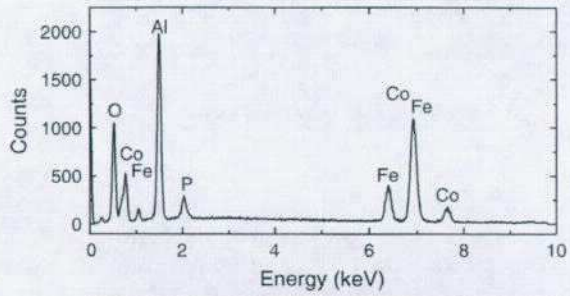

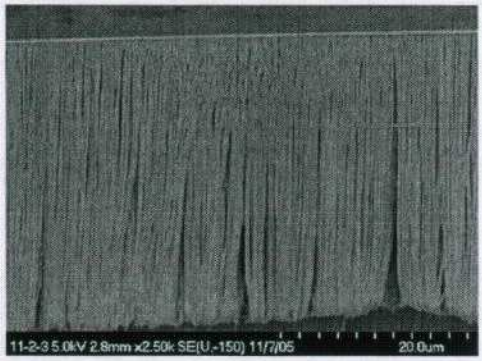

(a)

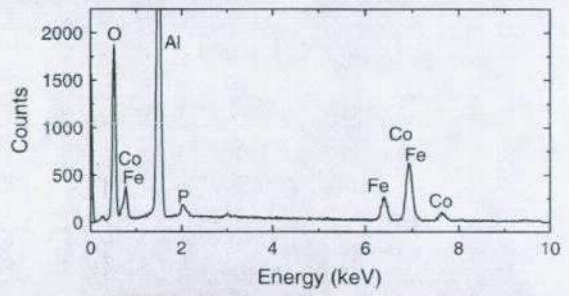

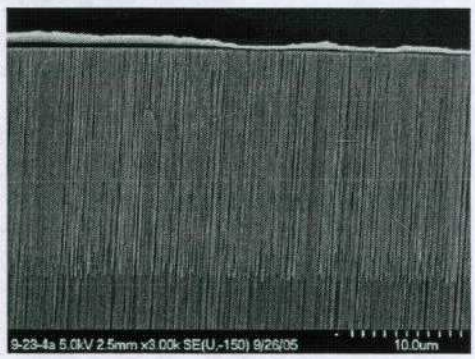

(b)

Fig. 2. EDX spectra (atop pictures) and SEM side views (lower images) of electrodeposited CoFeP nanowires after AAO templates were partly dissolved with 1 M NaOH solution: (a) deposited from a solution of pH = 3.2, with length of 31.1 μm; (b) deposited from a solution of pH = 4.0, with different length 20.8 μm. The two EDX patterns show that the nanowires consist of Co, Fe, P (Al on these diagrams comes from remains of the AAO).

In-plane hysteresis loops of each sample were fitted in the least square sense with analytical functions as defined by Eq. (3) with H_{k0} and σ as fit parameters. With these analytical functions, we obtain excellent fits of the

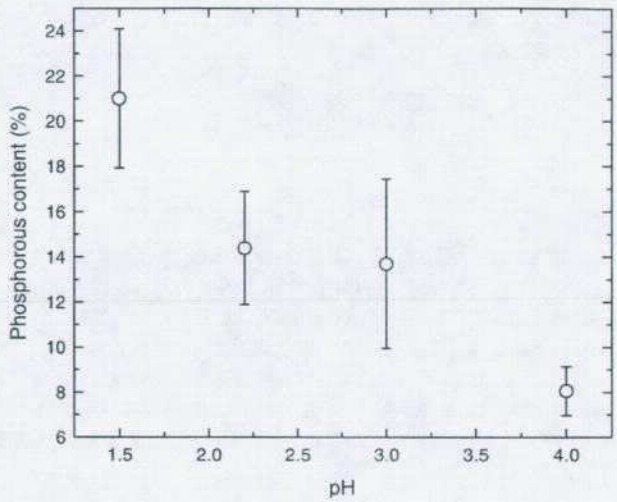

Fig. 3. Phosphorous content in the ferromagnetic alloy versus pH of the electrodeposition bath.

magnetization loops for all the samples investigated, confirming our hypothesis of log-normal distributions of particle anisotropy fields. In Figure 5 we show two extreme situations: large H_{k0} with small σ (open triangles) and small H_{k0} with large σ (open circles). In order to avoid the superposition of the branches at saturation, the magnetic moments of these loops were divided by two arbitrary and different values.

We may note several observations concerning the experimental hysteresis loops, and our analysis of them. First, H_{km} tends to increase with increasing pH of the electrodeposition bath. This is illustrated in Figure 6, in which we show the largest H_{km} observed for each series at constant pH but various electrodeposition times. While these samples do not have exactly the same value of l, the interaction field is not very different. Thus the variations in H_{km} originate rather in variations of $\tilde{h}_k$.

The experimental H_{km} values for arrays of different length but the same pH were fitted in the least square

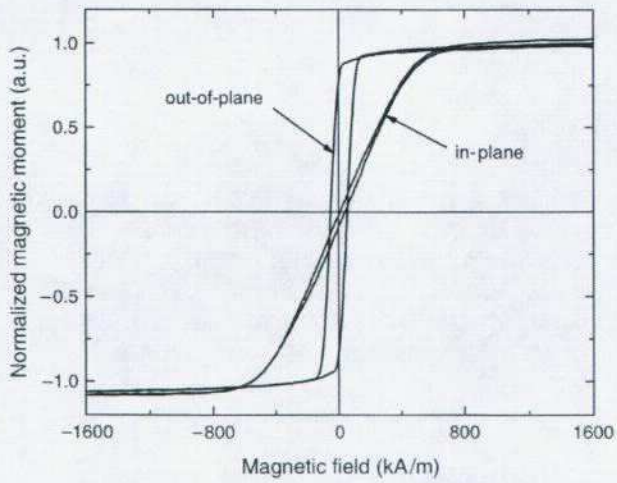

Fig. 4. In-plane and out-of-plane major hysteresis loops of a CoFeP nanowire array with average lengths of 25 μm obtained at pH = 3.0.

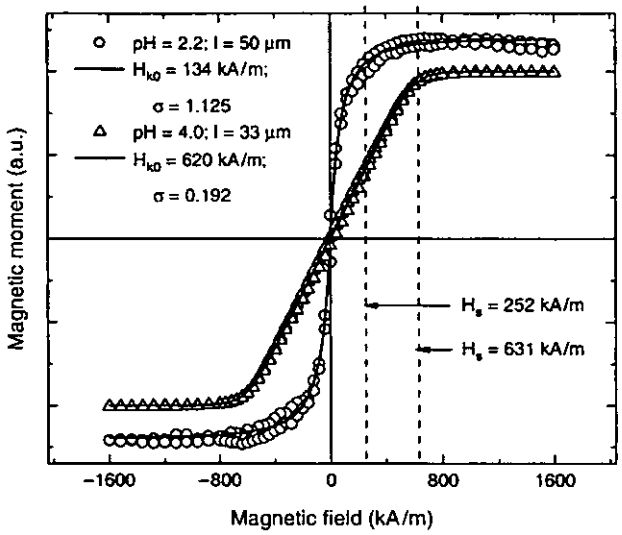

Fig. 5. Experimental (symbols) and theoretical (lines) in-plane major hysteresis loops for two nanowire arrays: pH = 2.2 with length of 50 μm (circles) and pH = 4.0 with length of 33 μm (triangles). H_{k0} and σ values for the best fit and are indicated in the figure legend. Vertical dashed lines indicate the lognormal mean of each distribution.

sense with linear functions and the corresponding slope and intercept used in Eq. (5) to evaluate the effective anisotropy field of the nanowires. The obtained values are shown in Figure 7. As we can see in this figure, the effective anisotropy field increases with the pH values. The magnitude of the error bars associated with the $\bar{h}_k$ values may originate either in the imprecision of the nanowires' length measurement or in the time variation of the bath electrodeposition parameters as well.

The increase in $\bar{h}_k$ with pH may be associated with the decrease in P content (as shown in Fig. 3) that causes an increase of the magnetization[23] but the intrinsic anisotropy may vary as well. In order to separate these

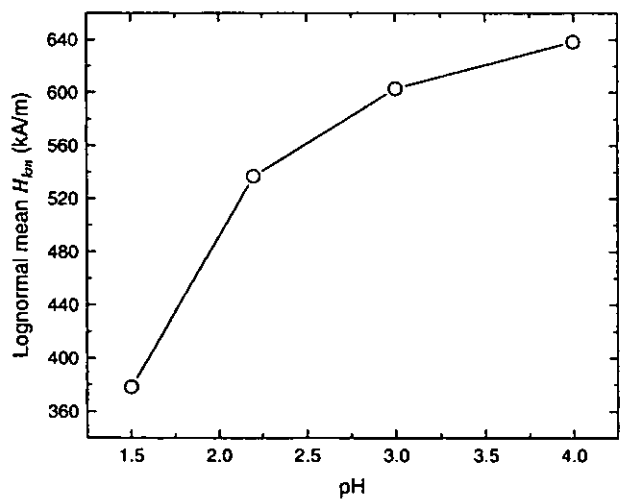

Fig. 6. Maximal values of the lognormal mean parameter, H_{km}, for nanowire arrays obtained at different values of the bath acidity.

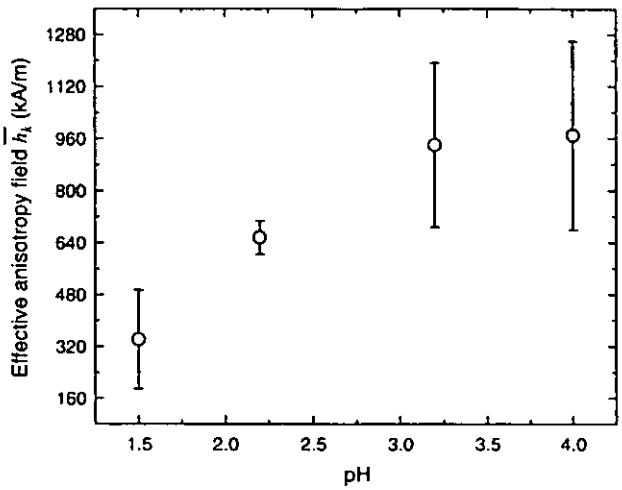

Fig. 7. Dependence of the effective anisotropy field $\bar{h}_k$ on the bath acidity.

accurately, we need a precise value of M_s, requiring accurate magnetometry and accurate determination of fill factor. If the intrinsic anisotropy is negligible with respect to the geometric anisotropy, we may extract M_s from Figure 7.

5. CONCLUSIONS

Amorphous CoFeP nanowire arrays were electrodeposited into the pores of home-made AAO membranes at different values of the bath acidity. EDX, XRD, and SEM techniques were used in order to evaluate the alloy phosphorous content and the average length of the nanowires respectively. The major hysteresis loops of these arrays were measured with a regular PPMS magnetometer. In-plane magnetization loops of CoFeP nanowire arrays were modeled with log-normal distributions of Stoner-Wohlfarth transverse magnetization loops and the influence of the bath acidity on the PDF log-normal parameters investigated for pH values from 1.5 up to 4.0. The fit of all the experimental loops is excellent. Using a phenomenological model for the interaction field at saturation and the PDF mean parameter as the saturation field of the array, we have quantitatively described the influence of bath acidity on the anisotropy fields in nanowires. Increasing pH leads to increasing anisotropy fields at least partly, due to demagnetization. Future investigations will deal with the stability of the bath parameters during the electrodeposition experiment, their influence on the homogeneity of the ferromagnetic nanowires, and with the relationship between the lognormal mean and the lognormal variance parameters.

Acknowledgment: This work is supported by a joint grant from the *Natural Sciences and Engineering Research Council* and the *National Research Council* of Canada.

RESEARCH ARTICLE

References and Notes

1. L. Piraux, S. Dubois, and J. L. Duvail, *J. Mater. Res.* 14, 3042 (1999).
2. N. Tsuya, T. Tokushima, M. Shiraki, Y. Wakui, Y. Saito, H. Kanamura, S. Hayano, A. Furugori, and M. Tanaka, *IEEE Trans. Magn.* 22, 1140 (1986).
3. S. Y. Chou, M. Wei, P. R. Krauss, and P. B. Fisher, *J. Vac. Sci. Technol. B* 12, 3659 (1994).
4. S. Y. Chou, P. R. Krauss, and L. Kong, *J. Appl. Phys.* 79, 6101 (1996).
5. M. Ciureanu, F. Béron, L. Clime, P. Ciureanu, A. Yelon, T. A. Ovari, R. W. Cochrane, F. Normandin, and T. Veres, *Electrochim. Acta* 50, 4487 (2005).
6. R. M. Metzger, V. V. Konovalov, M. Sun, T. Xu, G. Zangari, B. Xu, M. Benakli, and W. D. Doyle, *IEEE Trans. Magn.* 36, 30 (2000).
7. J. L. Duvail, S. Dubois, L. Piraux, A. Vaures, A. Fert, D. Adam, M. Champagne, F. Rousseaux, and D. Decanini, *J. Appl. Phys.* 84, 6359 (1998).
8. K. Hironaka and S. Uedaira, *IEEE Trans. Magn.* 26, 2421 (1990).
9. L. Clime, Thesis, University of Montreal (2005).
10. R. Hertel, *J. Appl. Phys.* 90, 5752 (2001).
11. R. Hertel, *J. Magn. Magn. Mater.* 249, 251 (2002).
12. G. J. Strijkers, J. H. Dalderop, M. A. A. Broeksteeg, and H. J. M. Swagten, *J. Appl. Phys.* 86, 5141 (1999).
13. R. Ferré, K. Ounadjela, J. M. George, L. Piraux, and S. Dubois, *Phys. Rev. B* 56, 14066 (1997).
14. M. Darques, A. Encinas, L. Vila, and L. Piraux, *J. Phys. Condens. Matter.* 16, S2279 (2004).
15. L. Clime, F. Béron, P. Ciureanu, M. Ciureanu, R. W. Cochrane, and A. Yelon, *J. Magn. Magn. Mater.* 299, 487 (2006).
16. H. Masuda and A. Fuduka, *Science* 268, 1466 (1995).
17. J. H. Yuan, F. Y. He, D. C. Sun, and X. H. Xia, *Chem. Mater.* 16, 1841 (2004).
18. J. Herreos, J. M. Barandiaran, and A. Garcia-Arribas, *J. Non-Crystalline Solids* 201, 102 (1996).
19. L. Clime, P. Ciureanu, and A. Yelon, *J. Magn. Magn. Mater.* 297, 60 (2006).
20. E. C. Stoner and E. P. Wohlfarth, *IEEE Trans. Magn.* 27, 3475 (1991).
21. J. C. Slonczewski, IBM Rept., RM003.111.224 (1956).
22. E. Limpert, W. A. Stahel, and M. Abbt, *Bio. Sci.* 51, 341 (2001).
23. N. V. Myung, D.-Y. Park, B.-Y. Yoo, and P. T. A. Sumodjo, *J. Magn. Magn. Mater.* 265, 189 (2003).

Received: 24 April 2006. Accepted: 28 May 2006.

RESEARCH ARTICLE